Movement Disorders (2015).
DOI: http://dx.doi.org/10.1002/mds.26201

Automated Neuromelanin Imaging as a Diagnostic Biomarker for Parkinson's Disease

Gabriel Castellanos, MD, MSc,[1,3] María A. Fernández-Seara, PhD,[1,3] Oswaldo Lorenzo-Betancor, MD, PhD,[2,3] Sara Ortega-Cubero, MD,[2,3] Marc Puigvert, BS,[6] Javier Uranga, BS,[4] Marta Vidorreta, PhD,[1] Jaione Irigoyen, MSc,[1,2,3,5] Elena Lorenzo, BS,[2] Arrate Muñoz-Barrutia, PhD,[4,8] Carlos Ortiz-de-Solorzano, PhD,[4] Pau Pastor, MD, PhD,[2,3,5,7†] and María A. Pastor, MD, PhD[1,3,5†*]

[1] *Neuroimaging Laboratory, University of Navarra, Pamplona, Spain*

[2] *Neurogenetics Laboratory, University of Navarra, Pamplona, Spain*

[3] *CIBERNED, Centro de Investigación Biomédica en Red de Enfermedades Neurodegenerativas, Instituto de Salud Carlos III, Madrid, Spain*

[4] *Cancer Imaging Laboratory, Center for Applied Medical Research (CIMA), University of Navarra, Pamplona, Spain*

[5] *Department of Neurology, Clínica Universidad de Navarra, University of Navarra School of Medicine, Pamplona, Spain*

[6] *Pulmonary Department, Clínica Universidad de Navarra, University of Navarra School of Medicine, Pamplona, Spain*

[7] *Department of Neurology, Hospital Universitari Mutua de Terrassa, University of Barcelona, Barcelona, Spain*

[8] *Bioengineering and Aerospace Engineering Department, University Carlos III of Madrid and Gregorio Marañon Health Research Institute, Madrid, Spain*

ABSTRACT: We aimed to analyze the diagnostic accuracy of an automated segmentation and quantifica-tion method of the SNc and locus coeruleus (LC) volumes based on neuromelanin (NM)-sensitive MRI (NM-MRI) in patients with idiopathic (iPD) and monogenic (iPD) Parkinson's disease (PD). Thirty-six patients (23 idiopathic and 13 monogenic *PARKIN* or *LRRK2* mutations) and 37 age-matched healthy controls underwent 3T-NM-MRI. SNc and LC volumetry were performed using fully automated multi-image atlas segmentation. The diagnostic performance to differentiate PD from controls was measured using the area under the curve (AUC) and likelihood ratios based on receiver operating characteristic (ROC) analyses. We found a significant reduction of SNc and LC volumes in patients, when compared to controls. ROC analysis showed better diagnostic accuracy when using SNc volume than LC volume. Significant differences between ipsilateral and contralateral SNc volumes, in relation to the more clinically affected side, were found in patients with iPD ($P = 0.007$). Contralateral atrophy in the SNc showed the highest power to discriminate PD subjects from controls (AUC, 0.93-0.94; sensitivity, 91%–92%; specificity, 89%; positive likelihood ratio: 8.4-8.5; negative likelihood ratio: 0.09-0.1 at a single cut-off point). Inter-val likelihood ratios for contralateral SNc volume improved the diagnostic accuracy of volumetric measurements. SNc and LC volumetry based on NM-MRI resulting from the automated segmentation and quanti-fication technique can yield high diagnostic accuracy for differentiating PD from health and might be an unbiased disease biomarker.

Key Words: Parkinson's; substantia nigra; neurome-lanin; magnetic resonance imaging; diagnosis

Funding agencies: Supported by the Fund for Health Research Foundation (FIS-ISCIII), Spanish Ministry of Economy and Competitiveness (reference: PI 13/02211); Spanish Ministry of Science and Innovation SAF2006-10126 (2006-2009), SAF2010-22329-C02-01 (2011-2013), and SAF2013-47939-R (to P.P.); project 061131 from the "Fundació La Marató de TV3" and by the UTE project FIMA, Spain (to P.P.). C.O.d.S. and A.M.B. were supported by Spanish Ministry of Economy and Competitiveness DPI2012-38090-C03-02 and TEC2013-48552-C2-1-R, respectively.

Relevant conflicts of interest/financial disclosures: M.A.P. has been also funded by CIBERNED, Centro de Investigación Biomédica en Red de Enfermedades Neurodegenerativas, Instituto de Salud Carlos III, Madrid, Spain and by the UTE project FIMA, Spain. There are no conflicts of interest.

[*] **Correspondence to:** Dr. María A. Pastor, Center for Applied Medical Research, University of Navarra, Pio XII, 55, 31008 Pamplona, Spain; mapastor@unav.es

[†] Authors M.A.P. and P.P. contributed equally to the study.

Parkinson's disease (PD) is a neurodegenerative disorder characterized by asymmetrical bradykinesia, rest tremor, and rigidity. Loss of neuromelanin (NM)-containing neurons in the SNc and locus coeruleus (LC) is characteristic in early PD stages.[1,2] Thus, in vivo identification of underlying SNc and LC degeneration based on NM-sensitive MRI (NM-MRI)[3-7] may help in the diagnosis of PD.

There are no validated MRI biomarkers to quantify the brainstem PD neurodegeneration,[8,9] and accurate manual segmentation of brainstem nuclei is indeed difficult owing to their irregular morphological characteristics.[6,9] Multi-image atlas-based segmentation is a promising approach given that it accounts for the inter-subject variability to obtain reliable segmentations.[10]

Neuropathological reports of patients with *LRRK2* and *PARKIN* mutations show marked neuronal loss in the SNc and LC, as observed in idiopathic PD (iPD).[11] The accuracy of the clinical diagnosis of PD is highly variable and genetic forms are relatively rare, thus the postmortem examination still remains the gold standard to confirm the diagnosis of PD. Therefore, we hypothesized that the inclusion of more homogeneous groups, such as PD subjects with monogenic forms, could help to identify the characteristic NM-pigmented cell loss in iPD.

We aimed to analyze the diagnostic accuracy of an NM-MRI-based completely automated method for segmentation and quantification of SNc and LC volumes for differentiating healthy subjects from PD patients previously screened for the most common PD genes in our population (*LRRK2* and *PARKIN*). We also explored possible differences between subgroups of patients.

Patients and Methods

Participants

The inclusion criterion for the patients was that they had been diagnosed with probable PD by a movement disorders specialist according to the UK Brain Bank criteria.[12] Clinical data, such as dexterity and disease duration, were obtained. The clinically most affected side was recorded as left, right, or bilateral when the patient reported an asymmetric onset of motor symptoms or a predominantly affected side. PD subjects were assessed taking their current dopaminergic treatment with the UPDRS-III being in the ON state. We excluded subjects with a Mini–Mental State Examination score (MMSE) $<$24/30, PD H & Y staging $\geq$ IV, subjects with substantial head movements at rest, claustrophobia, history of DBS, and medical or personal conditions that prevented the subject from undergoing an MRI exam.

Age-matched unrelated healthy subjects and spouses of affected PD subjects were recruited in the same center and from the community. Subjects suffering from a neurological disorder or with a positive family history of neurodegenerative disease were excluded. Clinical assessment and MRI scanning were performed on the same day. Written informed consent was obtained from every participant and the institutional ethics research review board approved the study. In order to classify PD patients according to their genetic background, all patients were genotyped for *LRRK2* and *PARKIN* mutations (Supporting Table 1).

MRI Scanning Protocol

All scans were performed in a 3-T Trio TIM MR scanner (Siemens, Erlangen, Germany), using a 12-channel head array. Images of the brainstem were obtained with an NM-sensitive imaging sequence, modified from a T1-weighted fast spin-echo sequence, as described previously,[3] to achieve a slightly higher resolution with the following parameters: repetition time/echo time, 600/15 ms, two-echo train length, 11 slices, 2.0-mm slice thickness, 0.2-mm gap, 512 $\times$ 408 acquisition matrix, field of view, 220 $\times$ 175 mm^2 (pixel size 0.43 $\times$ 0.43 mm^2, interpolated to 0.21 $\times$ 0.21 mm^2), bandwidth 110 Hz/pixel, four averages, and total scan time of 12 minutes (Supporting Information). Slices were perpendicularly oriented toward the fourth ventricle floor, using a previously acquired sagittal localizer and covered from the posterior commissure to the pons.

Automated Volume Measurements of NM-MR Images

NM-pigmented regions were automatically delineated (Fig. 1) using a reference atlas composed of 13 manually segmented NM-MR images[10] (Supporting Information). We calculated the segmentation accuracy and used a modified approach from two previous studies[4,6] to quantify the SNc and LC volumes (Supporting Information).

Statistical Analyses

Nonparametric receiver operating characteristic (ROC) curves were constructed for each group of patients and control subjects using the clinical diagnosis as the "gold standard." Then, logistic regression was used to estimate the effect of adding the LC volume to the contralateral SNc volume measurements on the classification accuracy. Given that a single optimal cut-off point varies depending upon the calculation method employed and its associated costs,[13,14] we calculated the sensitivity, specificity, and classification accuracy of more than one selected cut-off point on the nonparametric ROC curves of patients with iPD and applied these cut-off points to the SNc volume measurements of all PD patients combined. In

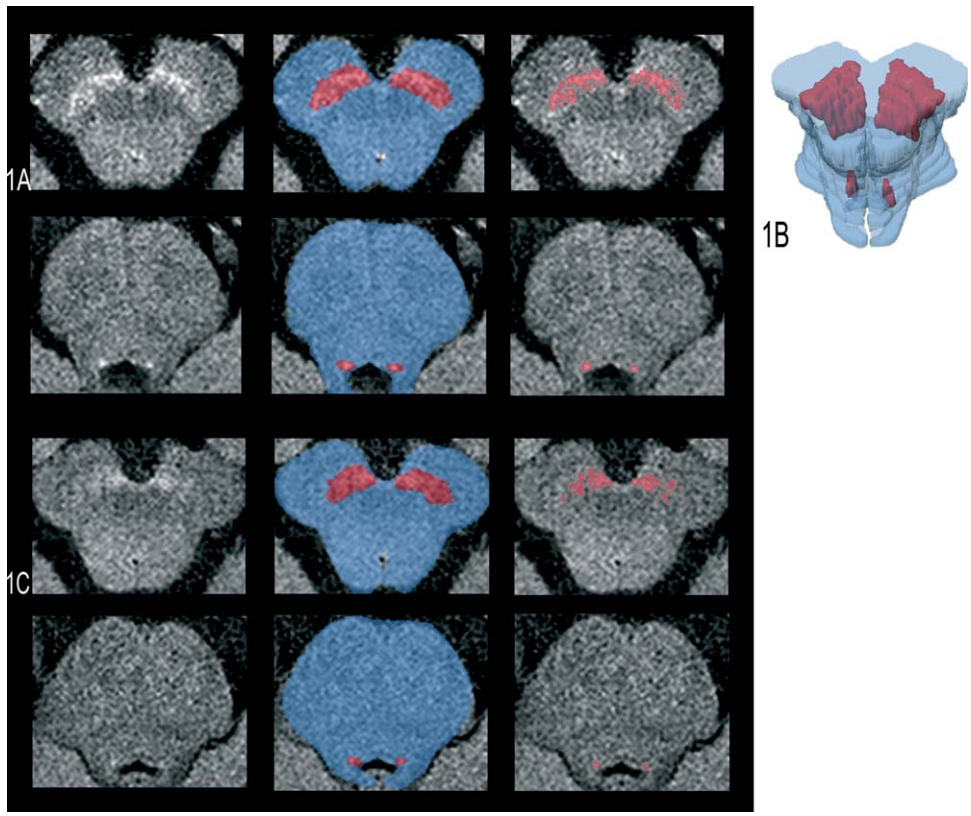

FIG. 1. NM-MRI showing the automatically segmented regions of interest (ROIs). SNc and LC of a healthy subject (A). Three-dimensional surface rendering corresponding to automated segmentation of the bilateral SNc and LC (B). NM-MRI of a patient with iPD with 4 years of motor symptom duration (C). NM-MR images of the SNc and LC (first column). ROIs detected in the automated segmentation with the brainstem background area shown in blue (second column). Hyperintense pixels of the SNc and LC above the threshold (third column).

addition, the positive and negative likelihood ratios (LR^+, LR^-) associated with the highest classification accuracy were computed. Using the same cut-off points, we constructed three categories as well as interval likelihood ratios (iLRs). iLRs have been suggested to assess the diagnostic value of tests with continuous measurements because they provide more-useful information.[15-17] We selected the optimal cut-off points by the ROC convex hull method (ROCCH).[18] Statistical analyses were performed using Stata software (12.0; StataCorp LP, College Station, TX) (Supporting Information).

Results

Demographic and Clinical Data

Thirty-six PD patients and 37 healthy subjects were recruited (Table 1). Thirteen (36%) patients showed a

TABLE 1. Demographic and clinical characteristics of the study groups

Characteristics	HS (n = 37)	iPD (n = 23)	PD *LRRK2* (n = 8)	PD *PARKIN* (n = 5)	*P* Value*
No. female/male	18/19	5/18	3/5	3/2	0.28[a]
Age, years	62 (52-70)	65 (55-70)	73 (67-75)	48 (47-67)	0.08
Handedness, right/left	37/0	22/1	7/1	5/0	NA
Most affected side, right/left/bilateral	NA	11/12/0	5/2/1	0/4/1	NA
Disease duration, years	NA	6 (3-8)	9 (7-10)	29[b,c](18-30)	<0.001
UPDRS-III Score	NA	13 (6-18)	12 (6-20)	19 (18-22)	0.07
MMSE Score	29 (28-30)	28 (27-29)	28 (25-29)	28 (25-30)	0.06

Data are presented as number or median (interquartile range).
*Kruskal-Wallis' test.
[a]Fisher's exact test.
[b]$P = 0.03$ (*PARKIN* vs. *LRRK2*).
[c]$P = 0.004$ (*PARKIN* vs. IPD).
HS, healthy subjects; PD *LRRK2*, *LRRK2* PD heterozygous mutation carriers; PD *PARKIN*, *PARKIN* PD mutation carriers; Disease duration, duration of motor symptoms for the more affected body side; UPDRS-III = UPDRS-motor scale; NA = not applicable.

TABLE 2. Bilateral volume measurements in the SNc and LC and comparisons between groups

Parameters	HS (n = 37)	iPD (n = 23)	PD *LRRK2* (n = 8)	PD *PARKIN* (n = 5)
SNc volume[a], mm^3	248.2 (214.3-284.6)	155.5 (124.5-188.9) $P < 0.001$[b] AUC = 0.91 (0.82-0.97)	162.8 (127.8-205.6) $P = 0.005$[b] AUC = 0.86 (0.61-0.98)	122.5 (108.3-126.0) $P = 0.002$[b] AUC = 0.97 (0.89-1.00)
LC volume[a], mm^3	15.2 (13.2-19.6)	11.9 (9.0-15.5) $P = 0.019$[b] AUC = 0.73 (0.58-0.86)	10.4 (7.9-13.0) $P = 0.002$[b] AUC = 0.88 (0.72-0.96)	8.2 (7.7-11.0) $P = 0.004$[b] AUC = 0.95 (0.84-1.00)

Data are presented as median (interquartile range).
[a]$P = <0.001$, comparison between all groups using Kruskal-Wallis' test.
[b]Compared with HS using the nonparametric Steel test.
HS, healthy subjects; PD *LRRK2*, *LRRK2* PD heterozygous mutation carriers; PD *PARKIN*, *PARKIN* PD mutation carriers; AUC, area under the ROC curve.

monogenic cause (5 patients carried mutations in the *PARKIN* gene and 8 in the *LRRK2* gene; Supporting Table 1). For the purpose of the study, patients were grouped in three categories based on *LRRK2/PARKIN* mutation status: (1) iPD; (2) combined *LRRK2* G2019S, R1441G, and R1761S carriers; and (3) combined *PARKIN* homozygotes and compound heterozygote.

Overall, 60% of the participants were male, but sex distribution did not significantly differ among the groups. A total of 34 (94%) patients reported an asymmetrical clinical course, affecting either the right or left side in 16 (44%) and 18 (50%) patients, respectively. Patients with *LRRK2* mutations were predominantly affected on the right side (5 of 8) and patients with *PARKIN* mutations on the left side (4 of 5). Median duration of motor symptoms in the total group of patients was 7 years. Although patients with *PARKIN* mutations had lower median age and higher median UPDRS-III scores, the differences between groups were not significant. The only statistically significant difference observed was the fact that *PARKIN* patients had an earlier age of onset and a longer duration of motor symptoms than the other groups (Table 1).

NM Imaging

Total SNc and LC volumes were significantly reduced in iPD patients and in those with *LRRK2* and *PARKIN* mutations, when compared to controls, and ROC curves indicated good classification performance for both markers and different thresholds (Table 2 and Supporting Table 2; Supporting Fig. 4). These measures demonstrated, on the one hand, similar discriminating power for both markers in patients with mutations and high discriminating power for identification of those with *PARKIN* mutations. On the other hand, the SNc showed better diagnostic accuracy than LC volume in iPD patients. In contrast, in a post-hoc analysis, we did not detect significant differences between patient subgroups.

When ipsilateral and the contralateral SNc volumes with reference to the clinically more affected side were compared (Fig. 2; Supporting Table 3), contralateral SNc volume was significantly reduced in patients with iPD by a mean difference of 12.8 mm^3 with respect to the ipsilateral side (95% confidence interval [CI] = 3.9-21.7 mm^3; paired t test: $t = 2.97$; $df = 22$; Hedges's $g = 0.50$; $P = 0.007$), but the differences did not reach statistical significance in monogenic PD (mPD) patients (mean difference = 11.9 mm^3; 95% CI = −0.5 to 24.5 mm^3; paired t test: $t = 2.13$; $df = 10$; Hedges's $g = 0.37$; $P = 0.059$). In the ROC analyses, higher AUCs for the contralateral SNc and

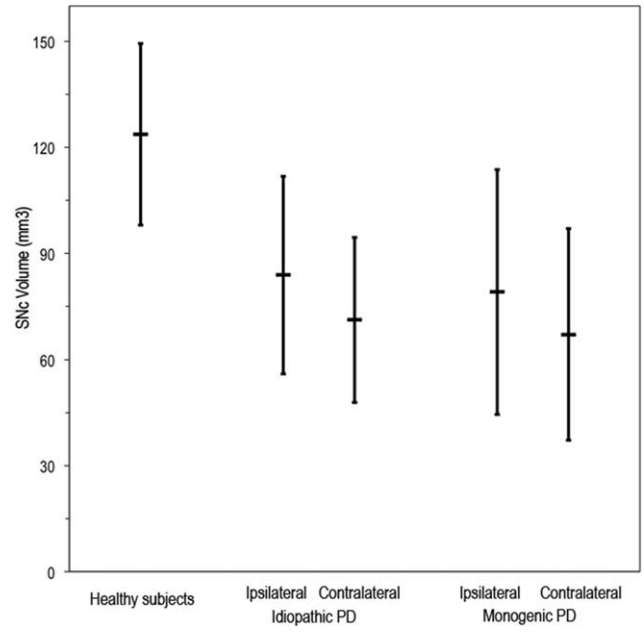

FIG. 2. Bar chart comparing the SNc volume measurements on NM-MRI in healthy subjects and groups of patients. Comparison of ipsilateral and contralateral SNc volume measurements in patients with iPD (n = 23) and in those with mPD (n = 11). Bars represent mean and error bars represent standard deviation. Volume contralateral to the clinically affected side was computed for patients with asymmetric disease and mean SNc volumes in the case of healthy subjects or patients with symmetric disease.

TABLE 3. Accuracy measures for contralateral SNc volume in PD patients

Cutoff (mm^3)	No. of HS	Patients with iPD (n = 23)	All PD patients (n = 36)	LR IPD	LR All PD patients
Single 103.1	33/37 Specificity % 89.2 (75.3-95.7)	21/23 Sensitivity % 91.3 (73.2-97.6)	33/36 Sensitivity % 91.7 (78.2-97.1)	$LR^+ = 8.4$ (3.6-21.6) $LR^- = 0.098$ (0.027-0.31)	$LR^+ = 8.5$ (3.7-21.6) $LR^- = 0.093$ (0.032-0.25)
Intervals					
<72.1	1/37	13/23	21/36	20.9 (3.1-160)	21.6 (4.8-124.8)
72.1-106.1	7/37	10/23	14/36	2.3 (1.03-5.7)	2.1 (0.97-4.52)
>106.1	29/37	0/23	1/36	0	0.035 (0.006-0.18)

Single = cut-off point at the level with highest classification accuracy (90%). The number of subjects with an SNc volume falling into each level is shown. Data in parentheses are 95% CIs. The interval LR is the probability of the defined volume interval when PD is present divided by the probability of the same volume interval when the disease is absent. The intervals were constructed from optimal cut-off points defining the convex hull of the ROC curve in iPD patients.
HS, healthy subjects; AUC, area under the ROC curve.

similar AUCs for patients with iPD and for all patients combined (Supporting Table 3; Supporting Fig. 9).

Correlation analyses of total SNc or LC volumes with age, disease duration, UPDRS-III, or MMSE scores yielded no significant associations in any of the groups, nor correlation between SNc and LC volume changes. In the regression analysis considering all PD patients, age, sex, and clinical disease duration significantly predicted a reduction of SNc volume contralateral to the clinically predominantly affected side ($F_{3,32} = 4.1$; $P = 0.01$; $R_2 = 0.16$), but only disease duration was significantly associated (b = −0.99; 95% CI = −1.69 to −0.28; $t(36) = -2.87$; $P = 0.007$). Despite this association, the results of parametric ROC analyses showed no significant influence of age, sex, or disease duration on the ROC curve, with an adjusted AUC of 0.93 (95% CI = 0.84-1.00), similar to the uncorrected model, which suggests that the power to discriminate between controls and PD patients tends to remain relatively stable across different disease durations. Addition of the LC volume to the contralateral SNc volume in a logistic regression model increased the AUC to 0.95 (Supporting Fig. 9).

ROC analysis showed that the best classification accuracy (90%) was obtained with a cut-off point of 103.1 mm^3 volume in the SNc, which resulted in high sensitivities and specificities in patients and controls (Table 3). With the SNc volume measurements dichotomized at this cut-off point, the LR^+ of a decrease in the volume was higher than 8 and the LR^- lower than 0.1. To further explore the possible diagnostic utility of SNc volume quantification, we calculated the iLRs for SNc volume measurements for iPD and all PD patients combined (Table 3). As expected, lower SNc volume measurements were associated with greater LRs (>20) and higher SNc volume measurements with lower LRs (<0.05). Intervals with higher and lower SNc volumes showed more informative LRs than LRs obtained using a single cut-off value.

Discussion

This study aimed to establish the diagnostic accuracy of quantification of structural brainstem changes in iPD and mPD using a T1-weighted NM-MRI optimized technique. The results of our study showed that the degree of SNc atrophy, measured using a fully automated quantification technique based on the NM-MR images, and especially the contralateral SNc volume to the most clinically affected side, had high discriminatory power to differentiate healthy subjects from patients with PD. This suggests that this measure has potential diagnostic utility in clinical settings, as well as for future studies including both idiopathic and monogenic forms of PD.

Our results are in agreement with previous NM-MRI studies in iPD with manual or semiautomatic segmentation methods, which have consistently reported significant reductions in measures of voxel intensity, area, and volume of total SNc and LC.[3-7]

We found higher diagnostic accuracy of the mean bilateral SNc at a single cut-off point when discriminating between PD patients and control subjects than previous NM-MRI studies,[6,7] possibly as a consequence of our fully automated volumetric method, suggesting that these assessments may have a potential diagnostic value. One previous study concluded that quantification of hyperintense pixels better reflects pigment content and was a more sensitive method.[4] Furthermore, owing to the asymmetrical nature of PD[19] and in vivo irregular morphological characteristics of these regions,[20] we modified previously proposed methods[4-6] and improved the quantification of hyperintense pixels by calculating an optimal threshold and by using an automated method. This allowed us to find not only significant total SNc and LC volume reductions, but also a reduction of the contralateral SNc volume relative to the clinically most affected side.

The ipsilateral versus contralateral SNc volume differences found in our study are in line with neuropathologic data[21] and also with previous neuroimaging studies, which have found asymmetries of the nigrostriatal system in patients with idiopathic and monogenic PD.[19,22-24] Previous MRI studies in PD have reported significantly lower T1 relaxation times[25] and higher iron deposition[26] in the contralateral SN to the most affected side, but not nigral atrophy. The

diagnostic accuracy of the ipsilateral SNc volume measurement was similar to previous studies using manual or semiautomatic segmentation methods, but the contralateral volume showed higher power to discriminate PD subjects from controls. However, differences in image acquisition parameters, image processing, ROI selection methods, and clinical characteristics of patients hinder the quantitative comparison of NM-MRI studies. We also found that quantifying the LC volume could have a small added value in the discriminatory ability of the measures, which adds new information to the findings established by previous work.[3,4,7,27]

Other advanced techniques, such as relaxometry,[28] diffusion tensor imaging (DTI),[27,29] and susceptibility-weighted imaging (SWI),[30] are capable of identifying brainstem nuclei changes and have been proposed as imaging biomarkers in PD.[9] Manual or semiautomatic identification of the SN and LC and voxel-wise methods have been used to characterize the amount and direction of water diffusion in affected tissues on DTI images and the amount of iron deposition with relaxometry and SWI images. One study using NM-MRI and DTI showed LC changes in PD patients with rapid eye movement sleep behavior disorder (RBD),[27] but to date, no direct studies have been performed that compare the accuracy for PD diagnosis between NM-MR imaging and these different imaging methods.

The first advantage of NM-MRI over other MRI techniques is that it allows a better delineation of the SNc, given that the hyperintense signal area correlates with NM-containing neuron density as described in a NM-MRI postmortem case study.[31] Second, detecting the atrophy of the contralateral SNc to the most clinically affected side may allow earlier diagnosis, as has been suggested by recent longitudinal PET studies.[32,33] Finally, other studies showed that NM-MRI may also help in detecting specific PD subgroups, such as patients with RBD,[27] and in distinguishing PD from atypical parkinsonian syndromes.[34,35]

It has been reported that the PD presymptomatic neurodegenerative process lasts for 2 to 40 years.[2,32] When the pathological process reaches the pontine tegmentum, between Braak's stages 2 and 4, loss of pigmented neurons has been observed in the SNc and the LC, further increasing in later stages.[2] Although the affection of the LC cells precedes that of the SNc, we found higher discriminative power for the SNc than LC in patients with iPD, which could be the result of insufficient imaging resolution or higher vulnerability of NM-pigmented neurons of the SNc, compared with the LC, as has been observed in postmortem studies.[1,11,36,37] We also corroborated postmortem studies in PD *LRRK2* and *PARKIN* mutation carriers,[11] finding significant differences in monogenic patients when compared to controls.

Early diagnosis of PD is often difficult and diagnostic accuracy ranges between 26% and 90% and improves as a function of expertise, medication response, and disease duration.[38-40] Genetic analysis is a tool to predict accurately underlying pathology in patients. In our patients, median disease duration was 7 years (range, 1-33), and, although disease duration was longer in patients with *PARKIN* mutations and was associated with the SNc volume reduction in the total group of patients with PD, we were not able to detect any effect of disease duration on the discriminating power of the regression models. Previous cross-sectional NM-MRI[4,5] and PET[41] studies described similar levels of linear correlation with disease duration, and a recent study[42] showed no significant differences in total neuronal density of the SNc, despite differences in disease duration, between *PARKIN* and iPD. The small effect of the disease duration may be explained by the nonlinear pattern of nigral cell loss described in longitudinal PET studies,[22] the high inter-individual variability described in postmortem volumetric studies,[43-45] and also by a recent postmortem study in iPD that described a highly variable reduction (33%–80%) in SNc-pigmented cells in the first 7 years postdiagnosis with a slower, less variable rate of degeneration after 10 years of disease progression.[46]

In our study, the iLRs calculated on the SNc volume values divided into three levels produced more useful clinical information than when dichotomized and could potentially overcome the limitations of deriving a single threshold on a continuous measurement.[14-17] LRs reflect how many times more likely a measurement level is in patients, in comparison to control subjects, and, in our study, a contralateral volume lower than 72.1 mm^3 was approximately 20 times more likely to belong to a PD patient than to a control subject. Conversely, a volume higher than 106 mm^3 was approximately 20 times more likely to belong to a control than to a patient. We suggest that deriving iLRs can improve the diagnostic utility of SNc volumetric analyses in future studies and contribute to the incorporation of quantitative NM-MRI test as a clinical diagnostic tool to help predict the probability of PD on an individual patient basis.[16,47]

To improve volumetric accuracy, we used higher spatial resolution than previous NM-MRI studies and we attempted to correct for motion artefacts by acquiring separate averages, repeating motion-corrupted acquisitions, and combining them offline after motion correction. Finally, we used an unbiased automated method for segmentation as well as a more sensitive method for quantification. The advantage of using automated over manual segmentation is that it allows us to measure the volume of the SNc and LC with high reliability and objectivity, thus eliminating interoperator variability, which is especially useful in

studies with a large cohort of subjects, as well as longitudinal and multisite studies. Specifically, using a multi-image atlas in the segmentation process incorporates intersubject variability in the segmentation, which, in turn, provides accurate results in heterogeneous populations. One other strong point of our study is that we accurately assessed the mutation status of patients, which improved the confidence in the relationship between the etiological diagnosis and the neuroimaging findings.

The first limitation is that NM-MR imaging typically uses low spatial resolution in the slice direction that also suffers partial volume effect and insufficient coverage, which may result in inaccurate volume calculations and lower segmentation accuracy in PD patients, especially in the LC, possibly owing to its smaller volume. As a consequence of the spatial resolution or the sample size of each patient group, we could not detect significant differences between idiopathic and genetic PD. Nevertheless, we were able to detect significant differences, when compared to controls, and our data are in agreement with postmortem and with other neuroimaging studies of patients with idiopathic and monogenic PD. Other limitations of our study are its cross-sectional design, the lack of autopsy data supporting the accuracy of our imaging methodology, and, because no disease controls were examined, the specificity of our findings to the differential diagnosis could not be determined. Finally, and as previously discussed, another potential limitation is the significant difference in disease duration between the patient groups. Further studies with a higher sample size and improved technique, in more specific subgroups such as patients with RBD[27] and psychiatric disorders,[48] will be required to acknowledge these limitations.

In conclusion, using automated quantification of the contralateral SNc atrophy and LR-based statistical methods, we found high discriminatory accuracy between patients with PD and healthy subjects, which may offer good diagnostic value in clinical settings and for the design of future clinical trials. Degeneration of melanized neurons is an important pathological hallmark associated with the motor signs of PD, and so NM-MRI-related measures are biomarkers that could contribute to improve the diagnostic accuracy of the disease, as well as help toward a better understanding of the heterogeneous clinical and pathological characteristics of idiopathic and monogenic PD. Ultimately, defining t he appropriate role for NM-MR imaging in the diagnosis and management of PD will require additional studies in order to further develop the method for future cohort studies including asymptomatic mutation carriers and patients with idiopathic and monogenic PD.

Acknowledgment: The authors are grateful to the families that participated in our studies.

References

1. Halliday GM, Ophof A, Broe M, et al. Alpha-synuclein redistributes to neuromelanin lipid in the substantia nigra early in Parkinson's disease. Brain 2005;128:2654-2664.
2. Braak H, Del Tredici K. Neuroanatomy and pathology of sporadic Parkinson's disease. Adv Anat Embryol Cell Biol 2009;201:1-119.
3. Sasaki M, Shibata E, Tohyama K, et al. Neuromelanin magnetic resonance imaging of locus ceruleus and substantia nigra in Parkinson's disease. Neuroreport 2006;17:1215-1218.
4. Schwarz ST, Rittman T, Gontu V, Morgan PS, Bajaj N, Auer DP. T1-weighted MRI shows stage-dependent substantia nigra signal loss in Parkinson's disease. Mov Disord 2011;26:1633-1638.
5. Kashihara K, Shinya T, Higaki F. Neuromelanin magnetic resonance imaging of nigral volume loss in patients with Parkinson's disease. J Clin Neurosci 2011;18:1093-1096.
6. Ogisu K, Kudo K, Sasaki M, et al. 3D neuromelanin-sensitive magnetic resonance imaging with semi-automated volume measurement of the substantia nigra pars compacta for diagnosis of Parkinson's disease. Neuroradiology 2013;55:719-724.
7. Ohtsuka C, Sasaki M, Konno K, et al. Changes in substantia nigra and locus coeruleus in patients with early-stage Parkinson's disease using neuromelanin-sensitive MR imaging. Neurosci Lett 2013; 541:93-98.
8. Wu Y, Le W, Jankovic J. Preclinical biomarkers of Parkinson disease. Arch Neurol 2011;68:22-30.
9. Lehéricy S, Sharman MA, Dos Santos CL, Paquin R, Gallea C. Magnetic resonance imaging of the substantia nigra in Parkinson's disease. Mov Disord 2012;27:822-830.
10. Artaechevarria X, Munoz-Barrutia A, Ortiz-de-Solorzano C. Combination strategies in multi-atlas image segmentation: application to brain MR data. IEEE Trans Med Imaging 2009;28:1266-1277.
11. Poulopoulos M, Levy OA, Alcalay RN. The neuropathology of genetic Parkinson's disease. Mov Disord 2012;27:831-842.
12. Hughes AJ, Daniel SE, Kilford L, Lees AJ. Accuracy of clinical diagnosis of idiopathic Parkinson's disease: a clinico-pathological study of 100 cases. J Neurol Neurosurg Psychiatry 1992;55:181-184.
13. Metz CE. Basic principles of ROC analysis. Semin Nucl Med 1978;8:283-298.
14. Zou KH, Yu CR, Liu K, Carlsson MO, Cabrera J. Optimal thresholds by maximizing or minimizing various metrics via ROC-type analysis. Acad Radiol 2013;20:807-815.
15. Dujardin B, Van den Ende J, Van Gompel A, Unger JP, Van der Stuyft P. Likelihood ratios: a real improvement for clinical decision making? Eur. J. Epidemiol. 1994;10:29-36.
16. Brown MD, Reeves MJ. Interval likelihood ratios: another advantage for the evidence-based diagnostician. Ann Emerg Med 2003; 42:292-297.
17. Grimes DA, Schulz KF. Refining clinical diagnosis with likelihood ratios. Lancet 2005;365:1500-1506.
18. Provost F, Fawcett T. Robust classification for imprecise environments. Mach Learn 2001;42:203-231.
19. Djaldetti R, Ziv I, Melamed E. The mystery of motor asymmetry in Parkinson's disease. Lancet Neurol 2006;5:796-802.
20. Lehéricy S, Bardinet E, Poupon C, Vidailhet M, François C. 7 Tesla magnetic resonance imaging: a closer look at substantia nigra anatomy in Parkinson's disease. Mov. Disord. 2014;13:1574-1581.
21. Kempster PA, Gibb WR, Stern GM, Lees AJ. Asymmetry of substantia nigra neuronal loss in Parkinson's disease and its relevance to the mechanism of levodopa related motor fluctuations. J Neurol Neurosurg Psychiatry 1989;52:72-76.
22. Nandhagopal R, Kuramoto L, Schulzer M, et al. Longitudinal progression of sporadic Parkinson's disease: a multi-tracer positron emission tomography study. Brain 2009;132:2970-2979.
23. Van de Loo S, Walter U, Behnke S, et al. Reproducibility and diagnostic accuracy of substantia nigra sonography for the diagnosis of Parkinson's disease. J Neurol Neurosurg Psychiatry 2010;81:1087-1092.

24. McNeill A, Wu RM, Tzen KY, et al. Dopaminergic neuronal imaging in genetic Parkinson's disease: insights into pathogenesis. PLoS One 2013;8:e69190.
25. Baudrexel S, Nürnberger L, Rüb U, et al. Quantitative mapping of T1 and T2* discloses nigral and brainstem pathology in early Parkinson's disease. Neuroimage 2010;51:512-520.
26. Martin WRW, Wieler M, Gee M. Midbrain iron content in early Parkinson disease: a potential biomarker of disease status. Neurology 2008;70:1411-1417.
27. García-Lorenzo D, Longo-Dos Santos C, Ewenczyk C, L et al. The coeruleus/subcoeruleus complex in rapid eye movement sleep behaviour disorders in Parkinson's disease. Brain 2013;136:2120-2129.
28. Du G, Lewis MM, Styner M, et al. Combined R2* and diffusion tensor imaging changes in the substantia nigra in Parkinson's disease. Mov Disord 2011;26:1627-1632.
29. Prodoehl J, Li H, Planetta PJ, et al. Diffusion tensor imaging of Parkinson's disease, atypical parkinsonism, and essential tremor. Mov Disord 2013;28:1816-1822.
30. Schwarz ST, Afzal M, Morgan PS, Bajaj N, Gowland PA, Auer DP. The "swallow tail" appearance of the healthy nigrosome—a new accurate test of Parkinson's disease: a case-control and retrospective cross-sectional MRI study at 3T. PLoS One 2014;9:e93814.
31. Kitao S, Matsusue E, Fujii S, et al. Correlation between pathology and neuromelanin MR imaging in Parkinson's disease and dementia with Lewy bodies. Neuroradiology 2013;55:947-953.
32. Kuramoto L, Cragg J, Nandhagopal R, et al. The nature of progression in Parkinson's disease: an application of non-linear, multivariate, longitudinal random effects modelling. PLoS One 2013;8:e76595.
33. Nandhagopal R, Kuramoto L, Schulzer M, et al. Longitudinal evolution of compensatory changes in striatal dopamine processing in Parkinson's disease. Brain 2011;134:3290-3298.
34. Matsuura K, Maeda M, Yata K, et al. Neuromelanin magnetic resonance imaging in Parkinson's disease and multiple system atrophy. Eur Neurol 2013;70:70-77.
35. Ohtsuka C, Sasaki M, Konno K, et al. Differentiation of early-stage parkinsonisms using neuromelanin-sensitive magnetic resonance imaging. Parkinsonism Relat Disord 2014;20:755-760.
36. Samaranch L, Lorenzo-Betancor O, Arbelo JM, et al. PINK1-linked parkinsonism is associated with Lewy body pathology. Brain 2010;133:1128-1142.
37. Hoogendijk WJ, Pool CW, Troost D, van Zwieten E, Swaab DF. Image analyser-assisted morphometry of the locus coeruleus in Alzheimer's disease, Parkinson's disease and amyotrophic lateral sclerosis. Brain 1995;118:131-143.
38. Hughes AJ, Daniel SE, Ben-Shlomo Y, Lees AJ. The accuracy of diagnosis of parkinsonian syndromes in a specialist movement disorder service. Brain 2002;125:861-870.
39. Marshall VL, Reininger CB, Marquardt M, et al. Parkinson's disease is overdiagnosed clinically at baseline in diagnostically uncertain cases: a 3-year European multicenter study with repeat [123I]FP-CIT SPECT. Mov Disord 2009;24:500-508.
40. Adler CH, Beach TG, Shill HA, et al. Low clinical diagnostic accuracy of early vs advanced Parkinson disease. Neurology 2014;83:406-412.
41. Lee CS, Schulzer M, de la Fuente-Fernández R, et al. Lack of regional selectivity during the progression of Parkinson disease. Arch Neurol 2004;61:1920-1925.
42. Doherty KM, Silveira-Moriyama L, Parkkinen L, et al. Parkin disease: a clinicopathologic entity? JAMA Neurol 2013;70:571-579.
43. German DC, Manaye K, Smith WK, Woodward DJ, Saper CB. Midbrain dopaminergic cell loss in Parkinson's disease: computer visualization. Ann Neurol 1989;26:507-514.
44. German DC, Manaye KF, White CL, et al. Disease-specific patterns of locus coeruleus cell loss. Ann Neurol 1992;32:667-676.
45. Eriksen N, Stark AK, Pakkenberg B. Age and Parkinson's disease-related neuronal death in the substantia nigra pars compacta. J Neural Transm Suppl 2009;73:203-213.
46. Kordower JH, Olanow CW, Dodiya HB, et al. Disease duration and the integrity of the nigrostriatal system in Parkinson's disease. Brain 2013;136:2419-2431.
47. Simel DL, Keitz S. Update: primer on precision and accuracy. In: Simel D, Rennie D, editors. *The Rational Clinical Examination: Evidence-Based Clinical Diagnosis*. New York: McGraw-Hill Medical; 2008:9-16.
48. Shibata E, Sasaki M, Tohyama K, et al. Use of neuromelanin-sensitive MRI to distinguish schizophrenic and depressive patients and healthy individuals based on signal alterations in the substantia nigra and locus ceruleus. Biol Psychiatry 2008;64:401-406.

Supporting Data

Additional Supporting Information may be found in the online version of this article at the publisher's web-site.